Supporting Information

Asymmetric diarylamine guests for host-guest system with stimulus-responsive room temperature phosphorescence

Jinzheng Chen, Faxu Lin, Guodong Liang, Huahua Huang*, Tian Qin*, Zhiyong Yang*, and Zhenguo Chi

Characterizations

Unless otherwise noted, commercial reagents were purchased from Bidepharm, Adamas (Tansoole platform) and Energy Chemical, and used without further purification. The dry solvents were dried and distilled before use by the literature methods. All reactions were performed under an inertia atmosphere unless otherwise specified. Flash chromatography was performed using silica gel (300–400 mesh). Analytical thin layer chromatography was performed on 0.20 mm silica gel HSGF-254 plates (Huanghai, China), and visualized under 254 or 365 nm UV light. Column chromatography was performed on 200-300 mesh silica gel (Huanghai, China). ^{1}H and ^{13}C NMR spectra were obtained at 25 °C on a Bruker Advance III 400 MHz nuclear magnetic resonance (NMR) spectrometer. Chemical shifts are reported in parts per million (ppm) with reference to TMS or residual nuclei in deuterated solvents [^{1}H NMR (CDCl$_3$): δ =7.26 ppm; ^{13}C NMR (CDCl$_3$): δ = 77.2 ppm]. Coupling constants (J) are denoted in Hz. Multiplicities are denoted as follows: s = singlet, d = doublet, dd = doublet of doublets, t = triplet, q = quartet, m = multiplet, br = broad. MALDI-TOF-MS spectra were recorded on an UltrafleXtreme MALDI-TOF/TOF instrument (Bruker Daltonics, Germany) equipped with a 355 nm Nd: YAG laser at the instrumental analysis and research center of Sun Yat-Sen University. UV-visible spectra were measured on a SHIMADZU UV-3600 UV-VIS-NIR spectrometer instrument, a mode of total reflection for the solid-state sample. Photoluminescence spectra were measured using a Shimadzu RF-5301PC spectrometer, a Horiba Scientific Fluorolog-3 spectrofluorometer or an Ocean Optics QE65 Pro with a 365 nm Rhinospectrum RhinoLED as the excitation source.

Phosphorescence spectra and mechanoluminescence spectra were recorded on Ocean Optics QE65 Pro. Time-resolved emission decay behaviours were studied with a Horiba Scientific Fluorolog-3 spectrofluorometer. The fluorescence quantum yields of the film and various crystals were determined by using a Horiba Scientific Fluorolog-3 spectrofluorometer equipped with a Horiba Scientific Quanta-φ calibrated integrating sphere. The molecular geometry optimizations were performed by using the time-dependent density functional theory (TD-DFT) method at the b3lyp/6-31g(d) level in the Gaussian 16 program. The spin-orbit coupling (SOC) constants were studied with the ORCA package performed on the ORCA 4.2.0 program with def2-TZVP basis set. Cyclic voltammetry (CV) curve was obtained from a VMP-300 multichannel potentiostat using a three-electrode electrochemical cell. The three electrodes were as follow: a Ag/AgCl (0.01 M in acetonitrile) electrode used as the reference, a platinum wire used as the working electrode, and a platinum sheet used as the counter electrode. Tetrabutylammonium hexafluorophosphate (0.1 M) in dichloromethane was used as the electrolyte. Sample solution was purged with Ar for 10 min before each measurement, with scan rate of 50 mV/s. The electrochemical potential was calibrated using the ferrocene/ ferrocenium (Fc/Fc^+) couple as an external standard. The conversion $E(Fc/Fc^+) = 0.63$ V versus the normal hydrogen electrode was used. The measured oxidation potential of Fc/Fc^+ was 0.41 V versus the $Ag/AgNO_3$ electrode. According to the onset oxidation potential of the CV curves, the HOMO was estimated based on the vacuum energy level of ferrocene (5.1 eV): $HOMO = -(E_{onset} - 0.41$ V$) -5.1$ eV.

pH-responsive process

At each time, the MDPA-Ph@DMAP (doping ratio: 1:100) sample was put into solutions with different pH values and stated for about 5 min (almost insoluble in solutions). Then, the sample was taken out from solutions and dried at 65 °C for about 10 min to remove the residual solution.

Ink preparation and printing process

Firstly, appropriate amount of the DCM/EtOH (v/v: 1:1) mixed solvent was used to dissolve the MDPA-Ph@DMAP (doping ratio: 1:100) sample and sodium carboxyethyl cellulose to prepare an ink paste. Secondly, screen printing different patterns were printed through screen printing technology or stamp process using prepared ink paste. The final samples for anti-counterfeiting applications could be obtained after the solvent volatilization.

General procedure for synthesis of guest compounds:

A suspension of bromide (4.0 mmol), *p*-anisidine (0.52 g, 4.2 mmol), Pd$_2$(dba)$_3$ (0.18 g, 0.2 mmol), dppf (0.11 g, 0.2 mmol) and NaO*t*Bu (0.38 g, 4.0 mmol) in 30 mL of dry toluene was stirred under nitrogen atmosphere for 24 h at 80 °C. After cooling to room temperature, the reaction mixture was concentrated. The residue was purified by chromatography on silica gel (eluting with hexane/CH$_2$Cl$_2$, 10/1 to 5/1 *v/v*) to give the corresponding guest.

MDPA-Ph[1], MDPA-PhBr[2], MDPA-FLU[3] are known and were identified by comparison of their NMR data with those reported in the literature.

The data of MDPA-Ph2: ^{1}H NMR (400 MHz, CDCl$_3$) δ 7.66 (d, *J* = 7.0 Hz, 10H), 7.48 (t, *J* = 7.4 Hz, 3H), 7.38 (m, *J* = 6.8 Hz, 2H), 6.93 (s, 2H), 3.85 (s, 3H). HR-ESI-MS *m/z* calcd. for C$_{25}$H$_{21}$NO [M+H]$^+$: 352.1690, found: 352.1692.
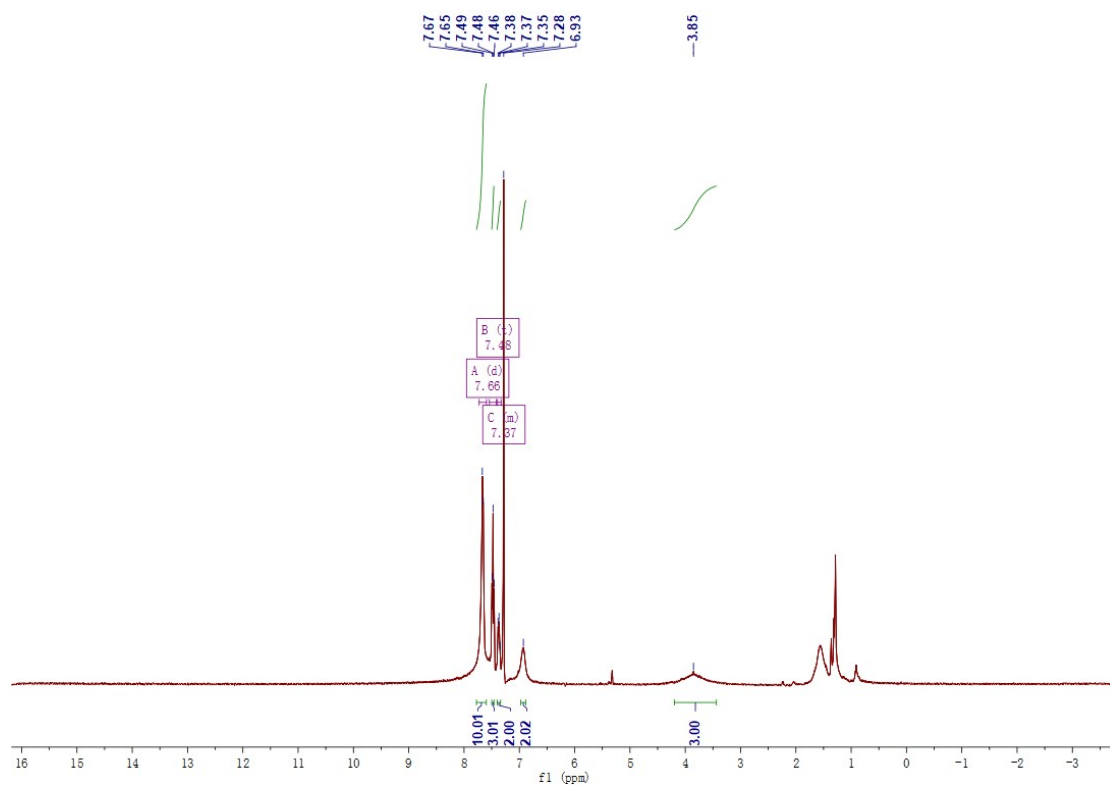
Fig. S1 ^{1}H NMR spectrum of MDPA-Ph2 (400 MHz, CDCl$_3$).
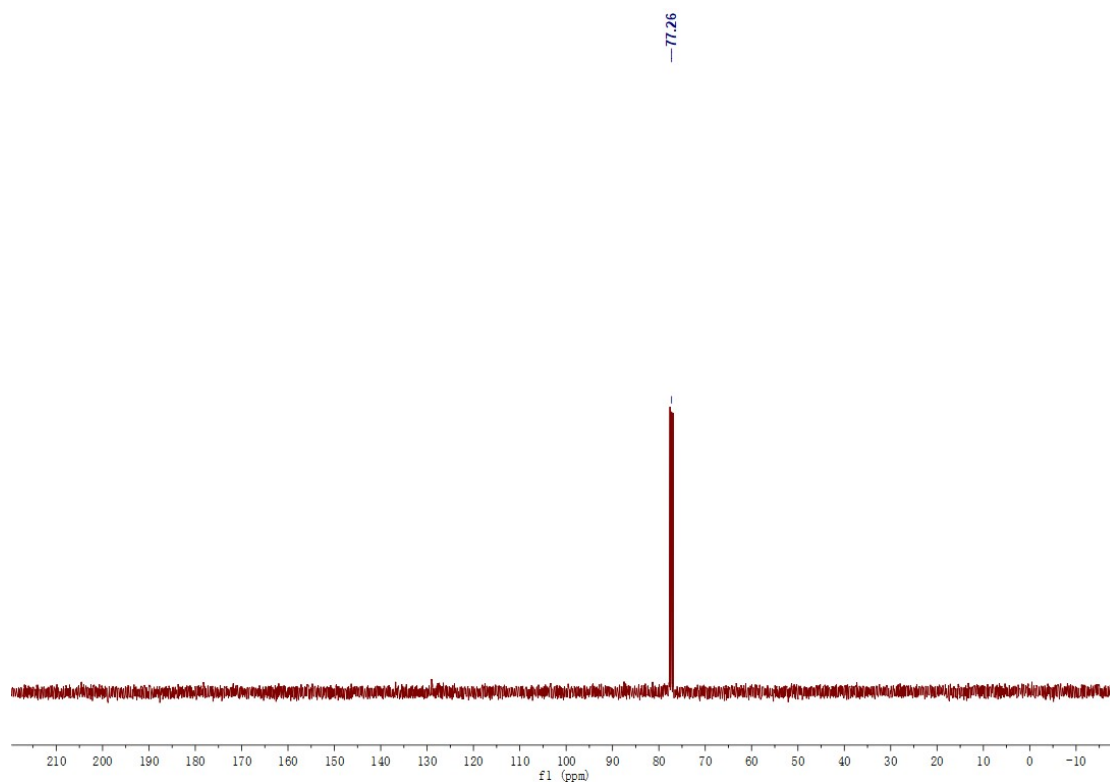
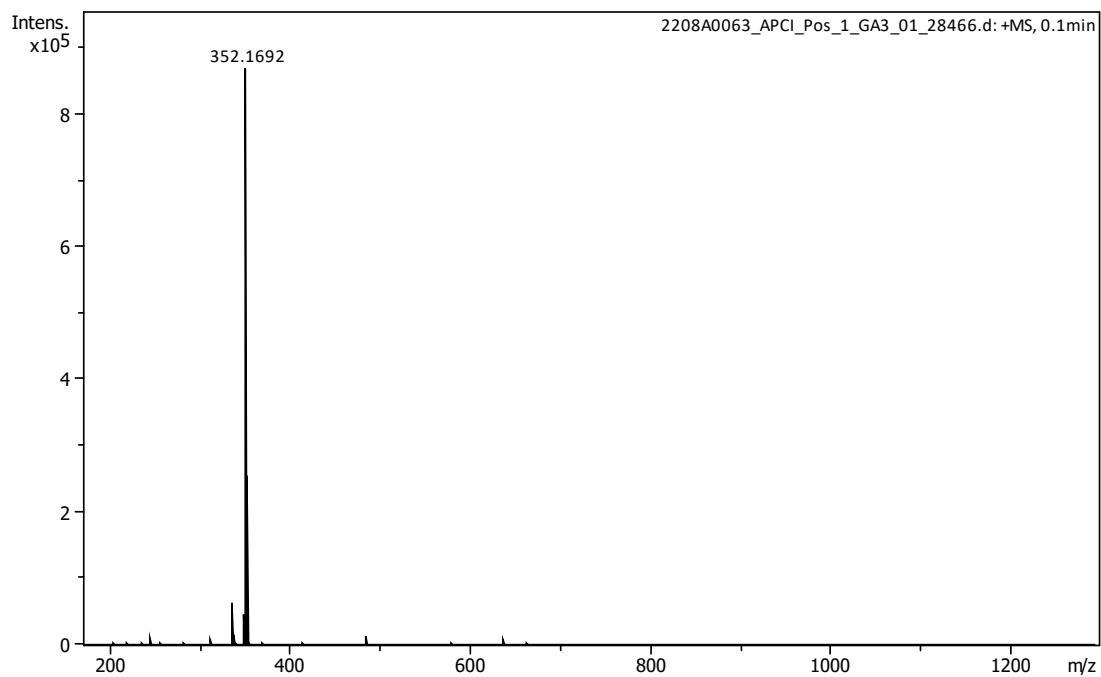**Fig. S2** ^{13}C NMR spectrum of MDPA-Ph2 (400 MHz, CDCl$_3$).

2208A0063_APCI_Pos_1_GA3_01_28466.d: +MS, 0.1min

352.1692

200   400   600   800   1000   1200   m/z

Fig. S3 HR-ESI-MS spectrum of MDPA-Ph2.

a)

Normalized intensity

MDPA
MDPA-Ph
MDPA-Ph2
MDPA-PhBr
MDPA-Flu

350   400   450   500
Wavelength (nm)

b)

Intensity (a.u.)

MDPA
MDPA-Ph
MDPA-Ph2
MDPA-PhBr
MDPA-Flu

400   500   600   700   800
Wavelength (nm)
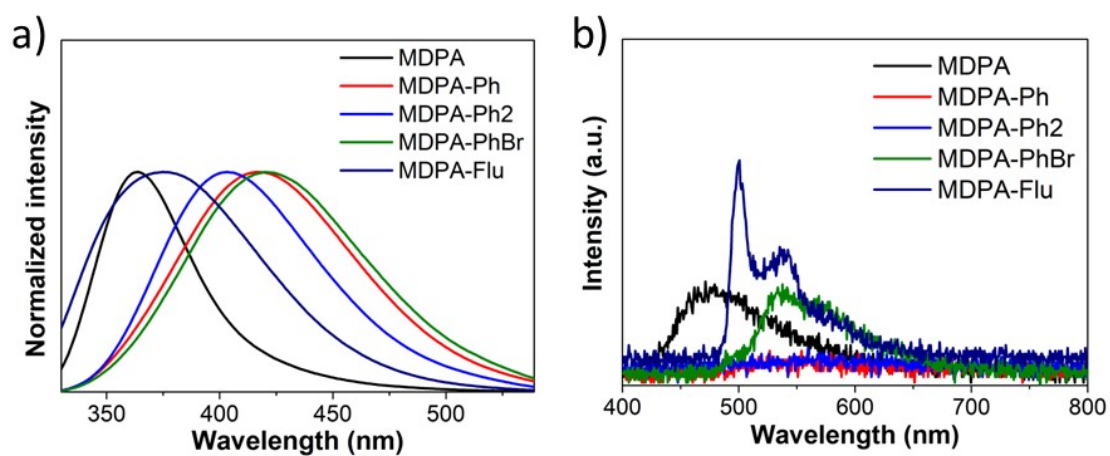
Fig. S4 a) Steady-state spectra of guests in diluted DCM solution at room temperature. b) Phosphorescence spectra of guests in diluted DCM solution at 77 K. Concentration: 1×10^{-5} mol/L.
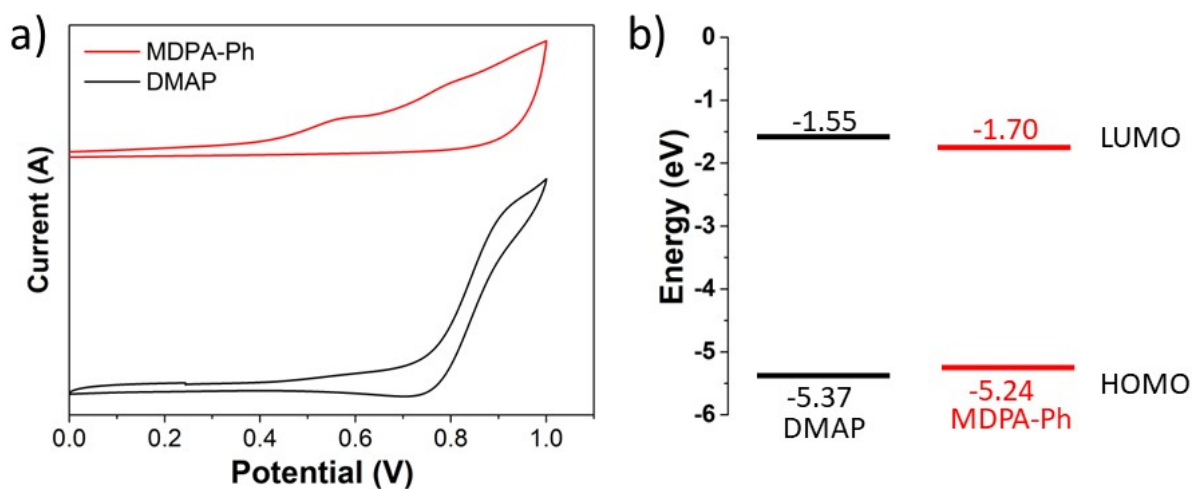
Fig. S5 a) Cyclic voltammograms of DMAP and MDPA-Ph measured in dichloromethane. b) Energy level diagrams for DMAP and MDPA-Ph.
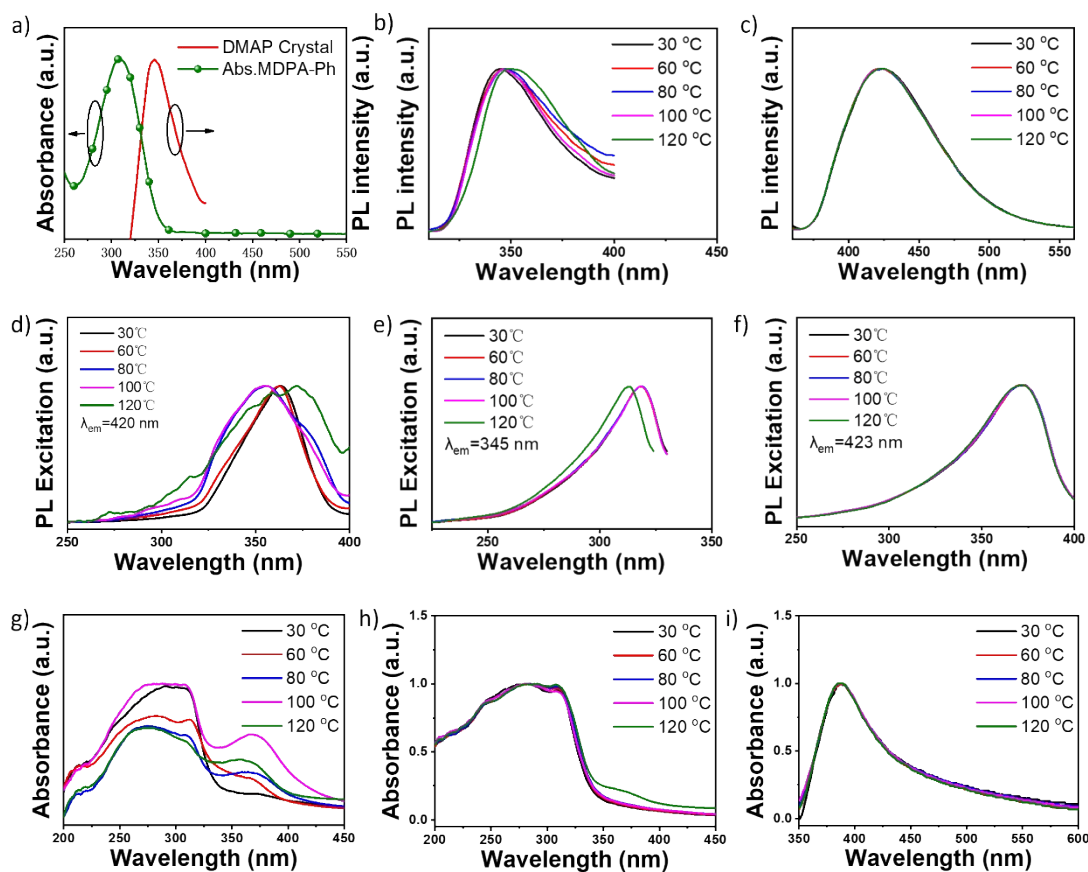
Fig. S6 a) Normalized fluorescence spectrum of DMAP crystal and UV-vis absorption spectrum of MDPA-Ph (in DCM solution, 10^{-5} M). A spectral overlap could be observed between the host emission and the guest absorption, which is essential for the FRET process; The fluorescence spectra of b) DMAP and c) MDPA-Ph after heating at different temperatures in solid-state; The fluorescence excitation

spectra of d) MDPA-Ph@DMAP, e) DMAP and f) MDPA-Ph after heating at different temperatures in solid-state; The absorption spectra of g) MDPA-Ph@DMAP, h) DMAP and i) MDPA-Ph at different temperatures in solid-state.
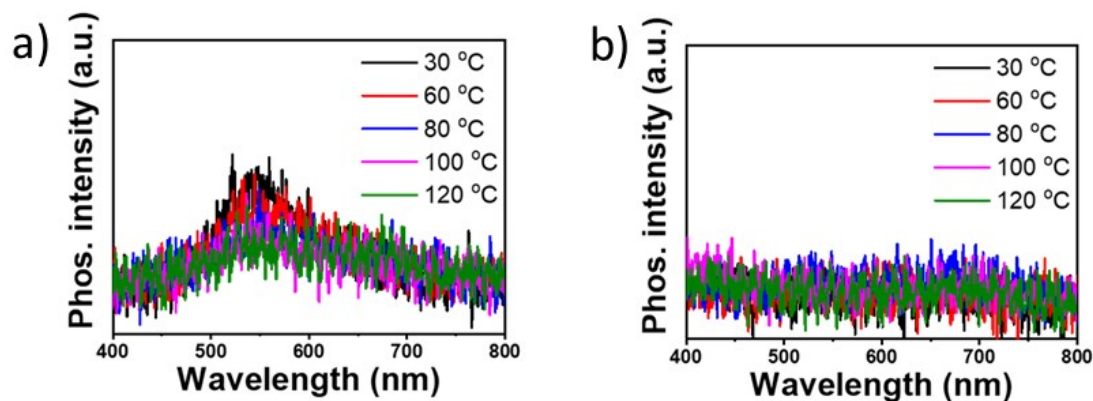
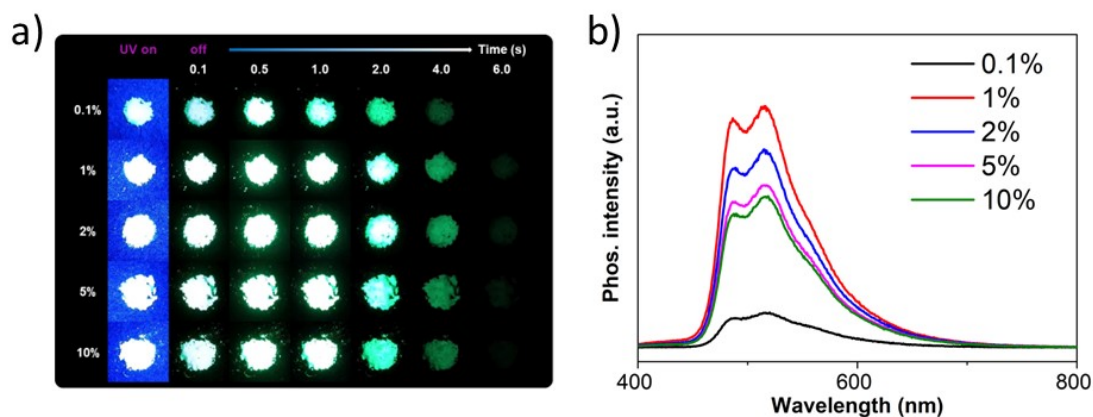**Fig. S7** Phosphorescence spectra of a) DMAP and b) MDPA-Ph at different temperature.

Fig. S8 a) Photographs of MDPA-Ph@DMAP doping samples with different guest ratios, a 365 nm UV lamp and after switching off the UV lamp. b) Phosphorescence decay curves of RTP in MDPA-Ph doping samples with different guest ratios.
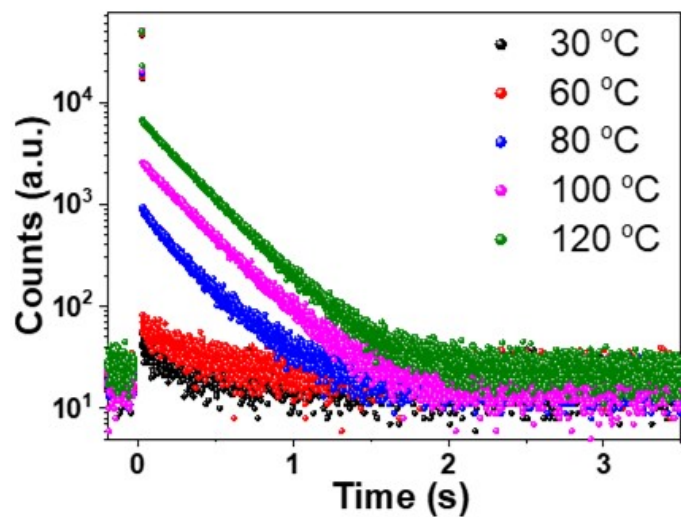
Fig. S9 Phosphorescence intensity decay curves of the heating-responsive RTP.
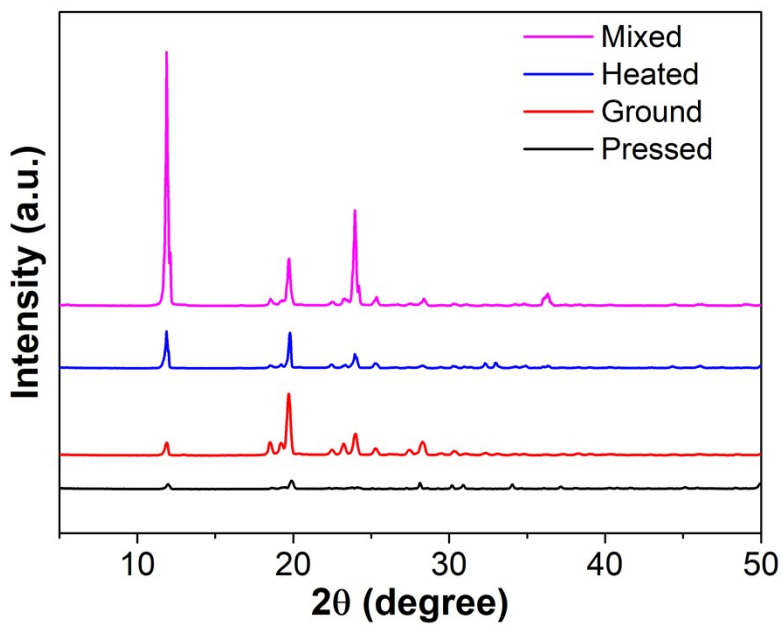

Fig. S10 The PXRD patterns of the MDPA-Ph@DMAP samples (Mixed, Heated, Ground and Pressed).
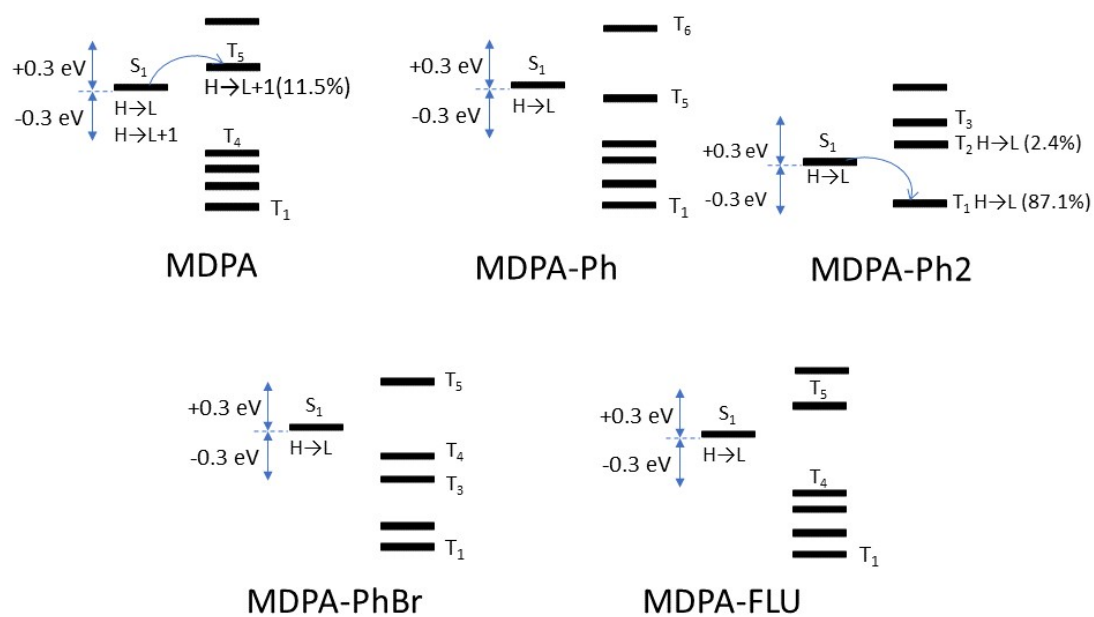
Fig. S11 The energy arrangements of guest molecules and possible transition channels for ISC transition.
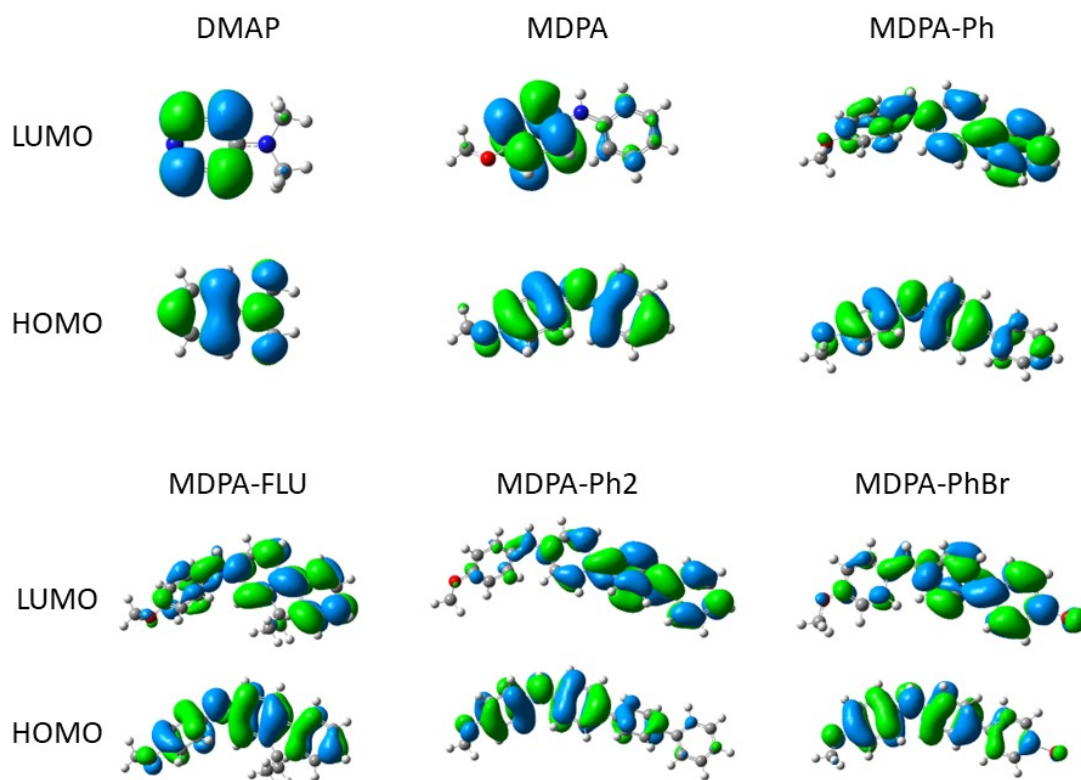

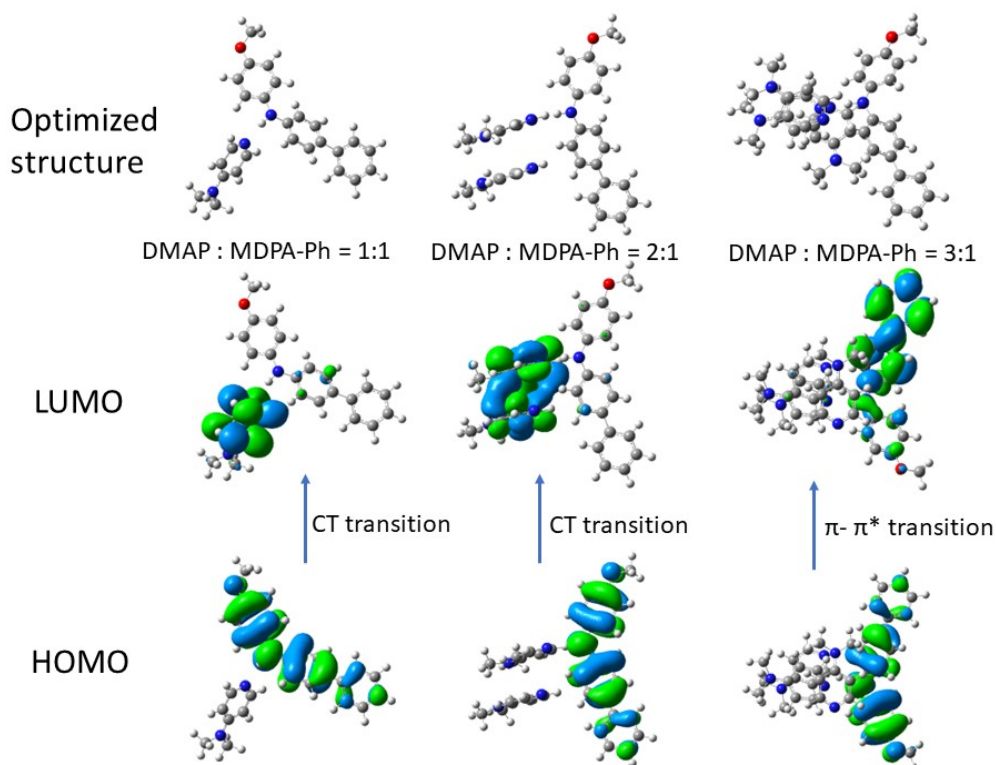**Fig. S12** The optimized structures and HOMO/LUMO distributions for DMAP and guests.

Fig. S13 The optimized structures and HOMO-LUMO distributions of MDPA-Ph@DMAP doping system with ratios from 1:1 to 3:1.
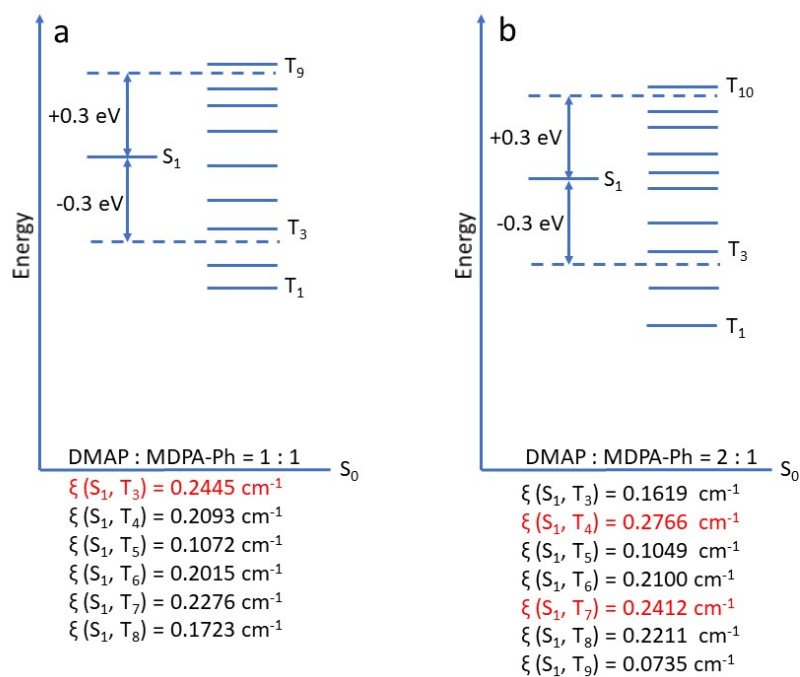

Fig. S14 Calculated spin-orbit coupling constants between S_1 and T_n for a) DMAP: MDPA-Ph = 1:1 and b) DMAP: MDPA-Ph = 2:1.
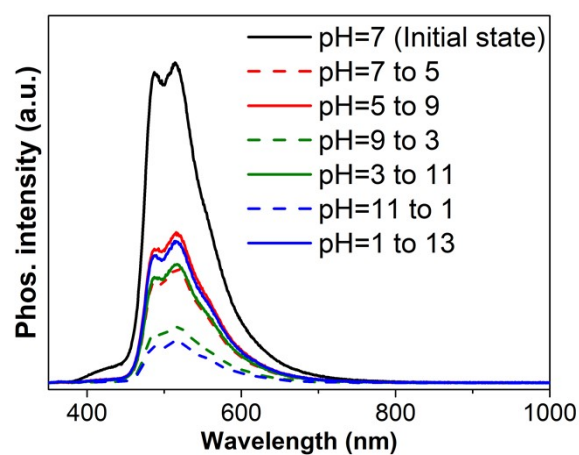
Fig. S15 The corresponding phosphorescent emission changes of MDPA-Ph@DMAP samples in different pH ranges.

Note and reference:

1 R. Takahashi, K. Kubota, H. Ito, *Chem. Commun.*, **2020**, 56, 407-410.

2 G. Li, L. Yang, J. J. Liu, W. Zhang, R. Cao, C. Wang, Z. Zhang, J. Xiao, D. Xue, *Angew. Chem. Int. Ed*., **2021**, 60, 5230-5234.

3 J.-Y. Shao, N. Yang, W. Guo, B.-B. Cui, Q. Chen, Y.-W. Zhong, *Chem. Commun*., **2019**, 55, 13406-13409.